

Midgap States and Generalized Supersymmetry in Semi-infinite Nanowires

Bor-Luen Huang¹, Shin-Tza Wu², and Chung-Yu Mou^{1,3}

1. *Department of Physics, National Tsing Hua University, Hsinchu 30043, Taiwan*

2. *Department of Physics, National Chung-Cheng University, Chiayi 621, Taiwan*

3. *National Center for Theoretical Sciences, P.O.Box 2-131, Hsinchu, Taiwan*

(Dated: October 25, 2018)

Edge states of semi-infinite nanowires in tight binding limit are examined. We argue that understanding these edge states provides a pathway to generic comprehension of surface states in many semi-infinite physical systems. It is shown that the edge states occur within the gaps of the corresponding bulk spectrum (thus also called the midgap states). More importantly, we show that the presence of these midgap states reflects an underlying generalized supersymmetry. This supersymmetric structure is a generalized rotational symmetry among sublattices and results in a universal tendency: all midgap states tend to vanish with periods commensurate with the underlying lattice. Based on our formulation, we propose a structure with superlattice in hopping to control the number of localized electronic states occurring at the ends of the nanowires. Other implications are also discussed. In particular, it is shown that the ordinarily recognized impurity states can be viewed as disguised midgap states.

PACS numbers: 73.20.-r, 73.20.At, 73.21.Hb

I. INTRODUCTION

The one-dimensional (1D) wire has been of great theoretical and experimental interests in the past. This is because of not only the wide variety of fascinating phenomena it exhibits, but also the testing grounds it offers for ideas that may become applicable in higher dimensions. In practice, 1D wires need not be physically one dimension. It may result from projection after a partial Fourier transformation from higher dimensional models. For instance, a superlattice structure can be reduced to an equivalent 1D structure after a partial Fourier transformation along the direction normal to the layers. Similar examples include *d*-wave superconductors, graphite sheet, and many other systems. Therefore, understanding the 1D wire is an ideal first step toward the understanding of any higher dimensional problems. Further boost for studying 1D wires comes from recent advances achieved in nanotechnology. Here the feasibility for bottom-up assembly of single nanowires¹ has made direct investigation of finite 1D wires possible. Nevertheless, conventional studies of the 1D wire have mostly been focused on its bulk properties, whereas assembled nanowires can only have finite lengths and must terminate at some sites (the ends, or the edges). It is therefore desirable to reconsider the effects of the ends to the properties of the nanowires.

The commonly recognized edge (or surface) effects in the physics of nanostructures are concerned with the large volume fraction of the boundaries. However, from either fundamental or practical viewpoints, the possible occurrence of edge modes and its influences on the properties of the system poses a much more interesting problem. For example, when applying carbon nanotubes as emitters for screen displays, the occurrence of edge states may change the density of electrons at the edge and thus affects the threshold working potential. It is therefore

of great technological interest if one could devise a way to engineer the number of edge states. From the fundamental viewpoint, the elegant role of edge excitations in the physics of Quantum Hall systems² is a well known example that illustrates the importance of edge states. Generally speaking, the edge states occur within the gap of the bulk energy spectrum and are called the midgap states. The existence of these states causes anomalous properties near the end which can manifest in tunneling measurements. A recently discovered example is the zero-bias conductance peak observed in the dI/dV measurement of the metal-*d*-wave superconductor junctions³. When electron-electron interactions are present, as occurs for an externally-implemented magnetic impurity, "intrinsic" Kondo effects may also arise due to these localized states, causing zero-bias anomaly near the Fermi energies⁴. Furthermore, if the system is finite, coupling between edge states can not be neglected. An example is the anomalous paramagnetic behavior observed in carbon nanoribbons⁵, where we have recently shown that there are residual antiferromagnetic couplings between edge spins in this system⁶. All these examples clearly illustrate the important role of edge states in the physics and applications of nanostructures.

In previous work, applying the Green's function approach, we have shown that broken reflection symmetry is a necessary condition for the occurrence of edge states, and the energies of edge states are the roots to the Green's function³. In this work, resorting to the supersymmetric method, we further develop a systematic way to determine the wavefunctions and the precise energies of the edge states.

Conventionally, the usage of the supersymmetric method in the condensed matter physics has been focused on applying the supersymmetry (SUSY) quantum field theory to disorder systems⁷. The application of the corresponding (0+1) dimensional limit -the SUSY quan-

tum mechanics⁸, however, is quite limited. Nevertheless, it has been realized⁹ that the zero-bias anomaly in d -wave superconductors is closely related with the SUSY quantum mechanics. These studies, however, are done in the continuum limit, using the semi-classical approximation, while the more relevant limit for high Tc superconductors and many other systems is the tight binding limit. Furthermore, the zero-energy state was the primary focus, while not all the states localized at the edge have zero energy. It is therefore important to see if the idea of SUSY quantum mechanics can be generalized to understand the finite-energy midgap states, in particular those in the discrete condensed matter systems, as well. In this work, we shall show that indeed, this is possible. We shall first show that the semi-infinite tight-binding d -wave superconductors belongs to a more general class, the bipartite system, and which can be well described by the conventional SUSY quantum mechanics⁸. Here the supersymmetric partners are two sublattices of the same system and the SUSY is characterized by a hermitian supercharge Q and the SUSY Hamiltonian $H^S = \{Q, Q\}/2$ with $[H^S, Q] = 0$. For bipartite systems with nearest neighbor hoppings, Q is identical to the physical Hamiltonian ($\equiv H_2$) and hence H^S is a quadratic functional of H_2 . Furthermore, the zero-energy state is annihilated by the supercharge, which then constitutes one of the conditions for determining the zero-energy state; while the other condition is to require it to decay from the edge. It is found that this conventional SUSY quantum mechanics can be appropriately extended to describe the semi-infinite p -partite systems with nearest neighbor hoppings. First, when $p \geq 3$, the original supercharge splits into two: In addition to the physical Hamiltonian H_p , a second supercharge Q_p can be formed. They both commute with the SUSY Hamiltonian H_S . Furthermore, only when $p = 2$, $H_S \approx H^S$ is a quadratic functional of H_p . In general, H_S is a polynomial functional of H_p . This is a reminiscence of the fractional SUSY quantum mechanics¹⁰ in which the SUSY Hamiltonian is generalized to be integer power of the supercharge. Nevertheless, our model is different and provides more realistic generalization of the conventional SUSY. The upshot of this generalization shows that, in addition to the zero-energy state, all the midgap states, including finite energy ones, are annihilated by the supercharge Q_p . The wavefunctions of the midgap states thus obtained tend to vanish with the same period commensurate with p : $\Psi_0 \approx (\dots, 0, \dots, 0, \dots, 0, \dots)$. These zeroes cut the original Hamiltonian into smaller ones so that the energies of the midgap states are determined by the eigenvalues of the Hamiltonian within each period. As a result, the matrix for determining the energies of midgap states is of size much smaller than the size of the original Hamiltonian. This reduction in matrix size heavily reduces the computation for determining the occurrence of the midgap states and provides a way to control the occurrence of the midgap states. As an application, we propose a structure with superlattice in hopping with period p to

control the number of localized electronic states occurring at the end of nanowires. In that case, the number of edge states is simply $p - 1$.

As the period p goes to infinity, the ensemble of configurations of hopping forms a semi-infinite disorder chain. This limit has been extensively investigated during the past¹¹ since Dyson's seminal work¹² in which it was pointed out that the average density of state (DOS) is enhanced at zero energy. From our point of view, this enhancement also reflects that the system has high probabilities to take the above-mentioned form for the ground state. The presence of the boundary breaks translational invariance. Thus, unlike the bulk case where the DOS at zero energy has no spatial dependence, the enhanced DOS at zero energy for semi-infinite disordered wires has the largest amplitude near the edge. Even for slight disorders, the effects of enhanced DOS at zero-energy are still observable. This offers a possible explanation for many unexpected zero-bias anomalies observed in tunneling experiments because, unless extremely carefully controlled, junction qualities are usually rather poor and disorders can easily set in near the junctions¹³.

Other implications and extensions of our generalized SUSY quantum mechanics will also be discussed. In particular, we shall demonstrate that by appropriate mappings, the ordinarily recognized impurity state can be viewed as a disguised midgap state. Such mapping provides a simple way to construct the impurity wavefunction and the corresponding energy. In addition to this application, possible extension to include the electron-electron interactions will also be discussed at the end of this paper.

This paper is organized as follows. In Sec.II, we lay down the basic tight binding model considered in this work and illustrate the SUSY quantum mechanics for the bipartite systems. In Sec.III, we generalize the supercharge and supersymmetric Hamiltonian to the p -partite systems and discuss the disorder limit. We also point it out of how to engineer the number of edge states by using a superlattice structure. By applying the SUSY quantum mechanics, we illustrate in Sec.IV how an impurity state can be viewed as a midgap state. In Sec.V, we conclude and discuss possible generalization to include electron-electron interactions. Appendices A and B are devoted to technical details of superalgebra and computation of commutators.

II. THEORETICAL FORMULATION AND SUPERSYMMETRIC QUANTUM MECHANICS

We start by considering the 1D atomic chain as illustrated in Fig. 1(a). This is the most general 1D atomic chain in which reflection symmetry with respect to the edge point is broken and, consequently, edge states might arise³. In the tight-binding limit, we consider the follow-

ing Hamiltonian to model this system: (a)

$$H_p = \sum_{i=1}^{\infty} t_i c_i^\dagger c_{i+1} + h.c. + v_i c_i^\dagger c_i. \quad (1)$$

Here the subscript p indicates the period of the lattice and i is the site index; t_i is the hopping amplitude between site i and its nearest neighbors, c_i (c_i^\dagger) is the electron annihilation (creation) operator, and v_i is the local potential at site i . We shall assume that both t_i and v_i are periodic with period p , namely $t_{p+i} = t_i$ and $v_{p+i} = v_i$. In real systems, this Hamiltonian may correspond to an assembly of p different atoms repeatedly arranged into a line (see Fig. 1). For wires composed of atoms of a single species, H_p may describe systems which exhibit density-wave order. This includes polyacetylene¹⁴, which has a dimerized structure and corresponds to $p = 2$, and polymers with higher commensurability charge density waves¹⁷. In the following, we shall call $p = 2$ the t_1 - t_2 model, and similarly for models with higher periods. As mentioned in the introduction, H_p may also represent the reduced model of a higher dimensional structure after partial Fourier transformation. For example, for a semi-infinite graphite sheet with zig-zag edge, since the system is translationally invariant along the edge, a partial Fourier transformation can be applied along this direction, leading to an effective 1D model. In this case, it is identical to the t_1 - t_2 model except that now t_1 and t_2 are k -dependent³: $t_1 = 2t_0 \cos(\sqrt{3}k_y a/2)$, $t_2 = t_0$, where a is the lattice constant and k_y represents the Fourier mode. This approach has been successfully applied to understand the anomalous properties near the edge in carbon ribbons⁶. As a final example, we note that the operator c_i in H_p needs not be restricted to be the electron annihilation operator. For example, after applying the Jordan-Wigner transformation, one can map a 1D quantum XY spin chain to a 1D model described by H_p . Specifically, we have t_i replaced by the exchange coupling for nearest neighbors $J_i/2$, and v_i replaced by the local magnetic field h_i . It is clear from these examples that H_p is quite general and captures the physics of many interesting systems.

To investigate the behavior of H_p near the edge, as a first step, we calculate the local density of states at the end point using the generalized method of image developed in Ref. 3. Fig. 2 shows typical local density of states at the end point for small periods. The parameters are carefully chosen so that all possible midgap states are present. In particular, we have set $v_i = 0$, which amounts to choosing the energy zero as the origin. These results show that midgap states are indeed the most prominent features at the end point. To understand how the midgap states arise, we first investigate the t_1 - t_2 model with $v_i = 0$ in details. In this case, since the lattice is bipartite, it is convenient to distinguish the amplitudes at the odd and the even sites by writing the wavefunction as $\Psi = (\phi_o, \phi_e)$. The Hamiltonian then

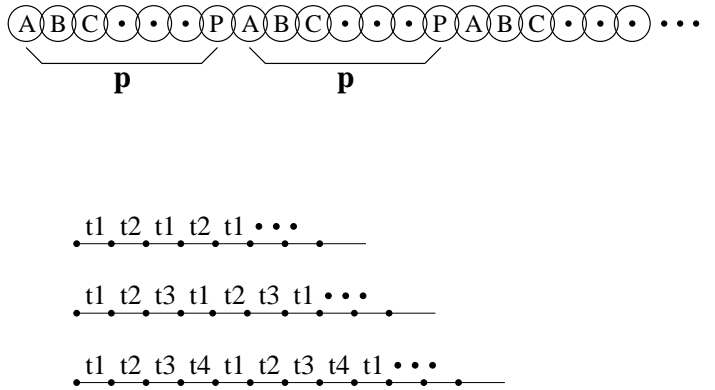


FIG. 1: Schematic plot of (a) an assembled atomic chain and (b) the corresponding models with small periods: $p = 2, 3$, and 4 .

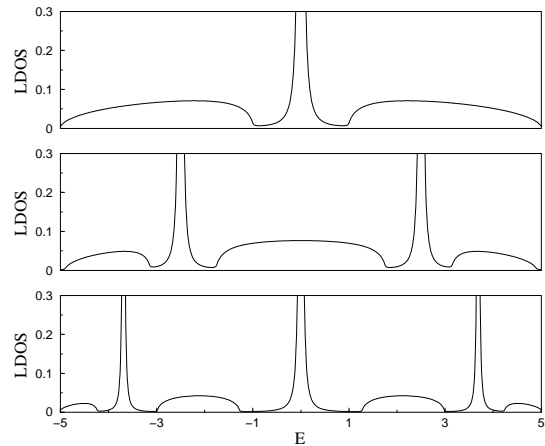


FIG. 2: The local density of states at the end point for small periods: $p = 2, 3$, and 4 . The parameters are carefully chosen so that the midgap states are manifested. Top: $t_1 = 2.0$, $t_2 = 3.0$ ($p = 2$); Middle: $t_1 = 2.5$, $t_2 = 1.8$, $t_3 = 3.0$ ($p = 3$); Bottom: $t_1 = 2.4$, $t_2 = 2.8$, $t_3 = 1.3$, $t_4 = 3.4$ ($p = 4$). All potential $v_i = 0$, and we have included a lifetime $\delta = 0.02$.

becomes

$$H_2 = \begin{pmatrix} \mathbf{0} & \mathbf{A} \\ \mathbf{A}^\dagger & \mathbf{0} \end{pmatrix}. \quad (2)$$

Here $\mathbf{0}$ is the null matrix and \mathbf{A} is a non-Hermitian matrix

$$\mathbf{A} = \begin{pmatrix} t_1 & 0 & 0 & \dots \\ t_2 & t_1 & 0 & \dots \\ 0 & t_2 & t_1 & \dots \\ \dots & \dots & \dots & \dots \end{pmatrix}. \quad (3)$$

It is interesting to note that the adjoint of \mathbf{A} satisfies

$$\mathbf{A}^\dagger = \varepsilon \mathbf{A} \varepsilon \quad \text{with} \quad \varepsilon = \begin{pmatrix} 0 & 0 & \dots & 1 \\ 0 & \dots & 1 & 0 \\ \dots & \dots & \dots & \dots \\ 1 & 0 & \dots & 0 \end{pmatrix}. \quad (4)$$

Here the operator ε effectively reflects the wavefunction with respect to the mid point of the lattice.

In the case of infinite chains, it is not hard to check that the corresponding matrices \mathbf{A} and \mathbf{A}^\dagger commute with each other and hence can be diagonalized simultaneously in Fourier space. For semi-infinite chains, however, \mathbf{A} and \mathbf{A}^\dagger do not commute and the spectrum of the t_1 - t_2 model can be best understood in terms of the supersymmetric quantum mechanics⁸. For this purpose, we first identify H_2 as the *supercharge* Q_2 , which connects even and odd sites. The block-diagonal matrix $(H_2)^2 (\equiv H^S)$ is then identified as (up to a factor of two) the corresponding supersymmetric Hamiltonian, whose diagonal blocks $H_o^S \equiv \mathbf{A}\mathbf{A}^\dagger$ and $H_e^S \equiv \mathbf{A}^\dagger\mathbf{A}$ are, respectively, the effective Hamiltonians for the odd and the even sites. Note that because \mathbf{A} and \mathbf{A}^\dagger do not commute, $H_o^S \neq H_e^S$. We will show below that the difference between H_o^S and H_e^S is the origin of the midgap states. Obviously, H^S is positive definite with the possibility when its spectrum touches zero. When the later happens, the ground state energy of H^S vanishes, the ground state wavefunctions ϕ_e and ϕ_o [$\Psi_0 = (\phi_o, \phi_e)$] have to be the zero-energy eigenfunction of \mathbf{A} and \mathbf{A}^\dagger , *ie.* $\mathbf{A}\phi_e = 0$ and $\mathbf{A}^\dagger\phi_o = 0$. In other words, the supercharge annihilates the ground state wavefunction Ψ_0

$$Q_2\Psi_0 = H_2\Psi_0 = 0. \quad (5)$$

Clearly, in this case, the system has good supersymmetry because the ground state is invariant under “rotation” between even and odd sites:

$$e^{i\theta Q_2}\Psi_0 = \Psi_0, \quad (6)$$

where θ is any real number. The non-Hermiticity of \mathbf{A} and \mathbf{A}^\dagger implies that forward and backward hopping amplitudes between two sites are different, and hence the eigenfunctions have to either grow or decay from the end point. Obviously, because of the relation $\mathbf{A}^\dagger = \varepsilon\mathbf{A}\varepsilon$, any non-trivial eigenfunctions satisfy $\phi_e = \varepsilon\phi_o$. Therefore, if ϕ_o decays from the edge, ϕ_e must grow from the edge (vice versa). For semi-infinite chains, only the even sites are connected with the hard-wall boundary point. Thus ϕ_e is forced to vanish while ϕ_o decays into the bulk, so that $\Psi_0 = (\phi_o, 0)$. Note that the other possible state $\Psi_0 = (0, \phi_e)$ resides on the other end of the chain and is pushed to infinity. Therefore, overall speaking, there is only half a chance for the existence of the ground state $(\phi_o, 0)$. This also reflects in the hopping strength difference. Indeed, we find that ϕ_o decays only when $t_1 < t_2$. In this case, H_o^S has a non-trivial zero energy eigenfunction, while H_e^S does not. Therefore, the system has good supersymmetry with *the ground state Ψ_0 being a localized state*. For finite energies, however, ϕ_e and ϕ_o need not be eigenfunctions of \mathbf{A} and \mathbf{A}^\dagger . Nevertheless, the supersymmetry allows a simple and elegant way to find the whole spectrum for the case $p = 2$. This is because H_e^S has the exact form as H_1 ($p = 1$) with $t_i = t_1t_2$

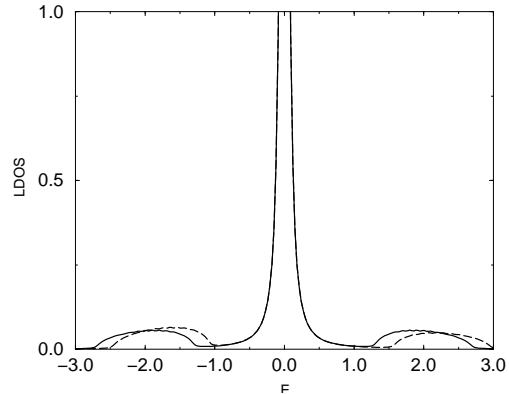


FIG. 3: The effect of the potential is to break the particle-hole symmetry so that two side bands are distorted. However, the midgap state is not changed if $v_o = 0$. The parameters are: $t_1 = 0.7$ and $t_2 = 2.0$. For solid line, $v_o = 0, v_e = 0$, while for dash line $v_o = 0, v_e = 0.5$.

and $v_i = (t_1^2 + t_2^2)$. Since this is just the ordinary uniform hopping model, one can easily write down the eigenstate: $\phi_e(n) = \sin 2nk$. The wavefunction at odd site can be then found by using the supercharge operator. We find that $\phi_o = \mathbf{A}\phi_e/E$ with E being the spectrum of H_2 which satisfies $E^2 = t_1^2 + t_2^2 + 2t_1t_2 \cos 2k$. Since $E^2 \geq (t_1 - t_2)^2$, an energy gap opens up around $E = 0$ when $t_1 \neq t_2$. In the case of $t_1 < t_2$, the ground state Ψ_0 then arises as a midgap state. Note that H_o^S is almost identical to H_e^S except for the potential energy $v_1 = t_1^2$ at the end point; the deficit energy t_2^2 is entirely due to the missing bond cut off by the boundary. We will elaborate on this in Sec.IV.

We now address the effects of the potential v_i . For $p = 2$, it is convenient to denote the potentials over the even sites v_e and the odd sites v_o . This decomposition, however, renders the particle-hole symmetry invalid at the level of the supercharge H_2 . Nonetheless, the spectrum (E) of H_2 can be mapped to the original spectrum of H^S with $v_i = 0$ ($\equiv E_S^0$). For $E_S^0 \neq 0$ this mapping is given by $E_S^0 = (E - v_e)(E - v_o)$, while for $E_S^0 = 0$, since $\phi_e = 0$ still holds, one has $E = v_o$. Hence even though the physical spectrum E may have no particle-hole symmetry, after appropriate transformations, the symmetric structure can be restored in E_S^0 ; in particular, the midgap state survives as clearly demonstrated in Fig. 3. For higher periods, the same manipulations as above can lead to similar conclusions. Therefore, unless explicitly needed, we shall ignore v_i in the following.

Let us now apply the supersymmetric method to semi-infinite superconductors⁹. After partial Fourier transformation along the interface, the problem becomes 1D superconductors with an end point. In this case, it is convenient to write the wavefunction by $\Psi = (u, v)$ with $u = (u_1, u_2, u_3, \dots)$ being particle-like and $v = (v_1, v_2, v_3, \dots)$ being hole-like wavefunctions. The reduced mean-field

(BCS) Hamiltonian is Dirac-like⁸ and can be generally written as

$$H_{BCS} = \begin{pmatrix} \mathbf{M} & \mathbf{Q} \\ \mathbf{Q} & -\mathbf{M} \end{pmatrix}, \quad (7)$$

where \mathbf{M} corresponds to the reduced 1D Hamiltonian for particles and \mathbf{Q} is essentially the pairing potential. One can also rewrite $H_{BCS} = \mathbf{M} \otimes \sigma_z + \mathbf{Q} \otimes \sigma_x$, and treat this problem as a spin in the ‘‘magnetic field’’ ($\mathbf{Q}, 0, \mathbf{M}$) pointing in the $x-z$ plane. This analogy suggests that it is possible to rotate the magnetic field to the $x-y$ plane. Indeed, this can be achieved by a rotation of $2\pi/3$ with respect to the axis $(1, 1, 1)$. The transformation matrix⁹ is

$$U = \frac{1}{\sqrt{2}} \begin{pmatrix} \mathbf{1} & \mathbf{1} \\ \mathbf{i} & -\mathbf{i} \end{pmatrix}, \quad (8)$$

where $\mathbf{1}$ and \mathbf{i} are semi-infinite matrices. The rotated Hamiltonian then takes the form of a supercharge like H_2

$$H'_{BCS} = U^\dagger H_{BCS} U = \begin{pmatrix} \mathbf{0} & \mathbf{M} - i\mathbf{Q} \\ \mathbf{M} + i\mathbf{Q} & \mathbf{0} \end{pmatrix}. \quad (9)$$

The wavefunction is rotated accordingly: $\Psi' = U^\dagger \Psi$. Therefore, in the supersymmetric form, particles and holes are mixed. As an illustration, we consider the mean-field Hamiltonian for d -wave superconductors

$$H_R = -\sum_{\langle ij \rangle, \sigma} t_0 c_{i\sigma}^\dagger c_{j\sigma} + \Delta_{ij} (c_{i\uparrow} c_{j\downarrow} - c_{i\downarrow} c_{j\uparrow}) + \text{h.c.} \quad (10)$$

where $\langle ij \rangle$ denotes the nearest-neighbor bonds, t_0 and Δ_{ij} are, respectively, the corresponding hopping and d -wave pairing amplitudes. For the $(1, 1, 0)$ interface, after Fourier transformation along the interface (which is taken to be the y direction), we obtain³

$$\mathbf{A} = \mathbf{M} - i\mathbf{Q} = \begin{pmatrix} -\mu & -t+d & 0 & \dots \\ -t-d & -\mu & -t+d & \dots \\ 0 & -t-d & -\mu & \dots \\ \dots & \dots & \dots & \dots \end{pmatrix}, \quad (11)$$

where μ is the chemical potential, $t = 2t_0 \cos(k_y a / \sqrt{2})$ and $d = 2\Delta_0 \sin(k_y a / \sqrt{2})$. The model for tight-binding d -wave superconductors is unique in the sense that the non-Hermiticity of \mathbf{A} and \mathbf{A}^\dagger can be removed by a gauge transformation. For this purpose, we write $t-d = \tilde{t}e^g$ and $t+d = \tilde{t}e^{-g}$ with $\tilde{t} = \sqrt{t^2 - d^2}$ and $e^{2g} = (t-d)/(t+d)$. The eigenfunction Ψ_E of \mathbf{A} is thus the gauge transformation of the eigenfunction ϕ_E of

$$\mathbf{A}_0 = \begin{pmatrix} -\mu & -\tilde{t} & 0 & \dots \\ -\tilde{t} & -\mu & -\tilde{t} & \dots \\ 0 & -\tilde{t} & -\mu & \dots \\ \dots & \dots & \dots & \dots \end{pmatrix}. \quad (12)$$

Specifically, we obtain $\Psi_E(n) = e^{-ng} \phi_E$ (for \mathbf{A}^\dagger , one obtains $\Psi_E(n) = e^{ng} \phi_E$). Furthermore, Ψ_E and ϕ_E have

the same eigenvalue E . This implies that the calculation of the zero mode is related to the spectrum of \mathbf{A}_0 . If we restrict our discussion to the propagating modes, the spectrum of \mathbf{A}_0 is simply the ordinary cosine band. We find that when $-2\sqrt{t^2 - d^2} < \mu < 2\sqrt{t^2 - d^2}$ is satisfied, \mathbf{A} and \mathbf{A}^\dagger can, respectively, support zero-modes of the form $(0, e^{-ng} \phi_{E=0})$ and $(e^{ng} \phi_{E=0}, 0)$. In this case, the ground state of H^S is selected by the sign of g , and thus the zero-energy midgap state is given by

$$u(n) = \frac{1}{\sqrt{2}} \left(\frac{t-|d|}{t+|d|} \right)^{n/2} \sin(k_F n a), \quad (13)$$

$$v(n) = \text{sign}(d) \frac{i}{\sqrt{2}} \left(\frac{t-|d|}{t+|d|} \right)^{n/2} \sin(k_F n a). \quad (14)$$

Here k_F is determined by $-2\sqrt{t^2 - d^2} \cos(k_F a) = \mu$ and depends on k_y ; therefore, even though the midgap states for different k_y 's have the same zero energy, their wavefunctions have k_y dependence. Note that for demonstration, we have only considered the case when k_F is real. Complete solutions, however, require to include the situation when k_F is complex¹⁵. In both cases, the supersymmetry structure enables one to write down the explicit form of the zero-energy mode near the interface $(1, 1, 0)$.

III. GENERALIZED SUPERCHARGE AND ITS CONSEQUENCES

We now generalize the above results to higher periods $p \geq 3$. It is useful to decompose the wavefunction as $\Psi = (\phi_1, \phi_2, \dots, \phi_p)$, where ϕ_n denotes the sub-wavefunction formed by $\{\Psi(kp+n); k=0, 1, 2, \dots\}$. The Hamiltonian is then cast in the form

$$H_p = \begin{pmatrix} \mathbf{0} & \mathbf{A}_{12} & \mathbf{0} & \dots & \mathbf{A}_{1p} \\ \mathbf{A}_{12}^\dagger & \mathbf{0} & \mathbf{A}_{23} & \dots & \mathbf{0} \\ \mathbf{0} & \mathbf{A}_{23}^\dagger & \mathbf{0} & \dots & \dots \\ \dots & \dots & \dots & \dots & \mathbf{A}_{p-1,p} \\ \mathbf{A}_{1p}^\dagger & \mathbf{0} & \dots & \mathbf{A}_{p-1,p}^\dagger & \mathbf{0} \end{pmatrix}. \quad (15)$$

Again, here $\mathbf{0}$ and \mathbf{A}_{nm} are block matrices; for all $n \neq p$, $\mathbf{A}_{nm} = t_n \mathbf{1}$ are diagonal, while for $(m, n) = (1, p)$

$$\mathbf{A}_{1p} = \begin{pmatrix} 0 & 0 & 0 & \dots \\ t_p & 0 & 0 & \dots \\ 0 & t_p & 0 & \dots \\ \dots & \dots & \dots & \dots \end{pmatrix}. \quad (16)$$

To understand what happens for the semi-infinite chain, it is useful to start from the infinite chain with Hamiltonian H_p^∞ . In this case, H_p^∞ also takes the same form except that \mathbf{A}_{nm} are further extended to $i = -\infty$. If we remove the hopping strength t_n and combine the remaining \mathbf{A}_{nm} with \mathbf{A}_{nm}^\dagger into \mathbf{Q}_{nm} for all m and n pairs, \mathbf{Q}_{nm} form a superalgebra if modulo p is performed (see Appendix A for mathematical details). The energy bands of H_p^∞ are determined by

$$P(E, k) = \det \begin{pmatrix} E & -t_1 e^{ik} & 0 & \dots & -t_p e^{-ik} \\ -t_1 e^{-ik} & E & -t_2 e^{ik} & \dots & 0 \\ 0 & -t_2 e^{-ik} & E & \dots & \cdot \\ \dots & \dots & \dots & \dots & -t_{p-1} e^{ik} \\ -t_p e^{ik} & 0 & \dots & -t_{p-1} e^{-ik} & E \end{pmatrix} = 0, \quad (17)$$

where E is the energy and k is the Fourier mode. In general, there have at most p energy bands. However, since in the polynomial $P(E, k)$, $(-1)^{p+1} 2t_1 t_2 t_3 \dots t_p \cos(pk)$ is the only term that depends on k , the function $P(E, k) - (-1)^{p+1} 2t_1 t_2 t_3 \dots t_p \cos(pk)$ maps p bands into one single band: $2t_1 t_2 t_3 \dots t_p \cos(pk)$. This important observation implies that when $H_p = H_p^\infty$, the operator $H_S \equiv P(H_p, 0) - (-1)^{p+1} 2t_1 t_2 t_3 \dots t_p$ is block-diagonal [there are p blocks with one for each ϕ_i , see Eqs.(B 1) and (B 2)] and folds the spectrum of H_p^∞ into one single band¹⁶. Therefore, H_S is similar to the supersymmetry Hamiltonian H_S . Indeed, for $p = 2$, we find $H_S = H_2^2 - (t_1^2 + t_2^2)$ which is essentially H^S .

For infinite chains, H_S is highly symmetric. In fact, it commutes with all Q_{mn} . This reflects that it is symmetric under the permutation of n and m but it is more than that because any linear combination of $\sum t_{mn} Q_{mn}$ also commutes with H_S . For semi-infinite chains, however, the above symmetry is broken: Not all Q_{mn} commute with H_S . Physically, this is obvious because now ϕ_p is special and is the only component that connects with the boundary point $i = 0$ directly. As a result, H_S is not completely block-diagonalized. In fact, because even for the infinite chains, $\phi_p(n) = \sin(knpa)$ is a solution for the p th block and it satisfies the hard-wall boundary condition at $i = 0$, the p th block is not affected. Therefore, there are only two blocks: one for the space formed by ϕ_p ; the other mixes ϕ_1, ϕ_2, \dots and ϕ_{p-1} . This is demonstrated in Eq.(B 1) where we denote the block Hamiltonians by \mathbf{H}^+ and \mathbf{H}^- .

Clearly, the t_1 - t_2 model is special because \mathbf{H}^+ and \mathbf{H}^- are of the same size so that H_S is completely block-diagonal. This is where the usual SUSY quantum mechanics applies. For $p \geq 3$, \mathbf{H}^+ and \mathbf{H}^- are not of the same size, a generalization of SUSY quantum mechanics is needed. First, it is important to see if one can find an operator, similar to the supercharge Q_2 , that commutes with H_S . H_p is obviously a solution because $H_2 = Q_2$. However, in analogy to the case of $p = 2$, a second supercharge by collecting all block matrices in H_p that connects ϕ_p to other components can be formed:

$$Q_p = \begin{pmatrix} \mathbf{0} & \mathbf{0} & \dots & \dots & \mathbf{A}_{1p} \\ \mathbf{0} & \mathbf{0} & \dots & \dots & \mathbf{0} \\ \dots & \dots & \mathbf{0} & \dots & \dots \\ \dots & \dots & \dots & \dots & \mathbf{A}_{p-1,p} \\ \mathbf{A}_{1p}^\dagger & \mathbf{0} & \dots & \mathbf{A}_{p-1,p}^\dagger & \mathbf{0} \end{pmatrix} \quad \text{for } p \geq 3. \quad (18)$$

Note that the above definition can also include $p = 2$. In that case, one squeezes the block \mathbf{A}_{1p} into \mathbf{A}_{12} to obtain the form of H_2 in Eq.(2). Because $\mathbf{A}_{12} = t_1 \mathbf{1}$ and \mathbf{A}_{1p} is given by Eq.(16) with t_p being replaced by t_2 , adding \mathbf{A}_{12} and \mathbf{A}_{1p} reproduces \mathbf{A} defined in Eq.(3) precisely. Hence Eq.(18) can be regarded as an "analytical continuation" of Q_2 to $p \geq 3$. Furthermore, as shown in Appendix B, $[H_S, Q_p] = 0$ is satisfied, thus Q_p provides a faithful generalization of Q_2 . It coincides with H_p only when $p = 2$. Note that from Appendix B, one can actually see that out of Q_{mn} contained in H_p , Q_p and H_p (and their linear combinations) are the only two generators that commute with H_S for general p .

Applying the condition that the supercharge annihilates midgap states Ψ_0 , one finds that

$$\phi_p = 0 \quad \text{and} \quad \mathbf{A}_{1p}^\dagger \phi_1 + \mathbf{A}_{p-1,p}^\dagger \phi_{p-1} = 0. \quad (19)$$

$\phi_p = 0$ implies that the wavefunction has the form $\Psi_0 \approx (\dots, 0, \dots, 0, \dots, 0, \dots)$ as pointed out earlier¹⁸, while the second condition relates ϕ_{p-1} to ϕ_1 . It is important to realize that because Q_p no longer coincides with H_p for $p \geq 3$, Q_p alone does not determine the energies and wavefunctions of the midgap states. Instead, because $Q_p \Psi_0 = 0$, the operator $H_p - Q_p$ determines the energies and further provides relations between $\phi_2, \dots, \phi_{p-1}$ and ϕ_1 . This analysis shows that the energies E_m of midgap states can be different from zero and must satisfy

$$\det \begin{pmatrix} -E_m & t_1 & 0 & \dots & 0 \\ t_1 & -E_m & t_2 & \dots & 0 \\ 0 & t_2 & -E_m & \dots & \cdot \\ \dots & \dots & \dots & \dots & t_{p-2} \\ 0 & 0 & \dots & t_{p-2} & -E_m \end{pmatrix} = 0. \quad (20)$$

Therefore, there are at most $p - 1$ midgap states. To stabilize the midgap states, one further requires Ψ_0 to decay away from the edge. In the case of $p = 2$, this results in the condition $t_1 < t_2$. For $p = 3$, one first obtains from Eq.(20) $E_m = \pm t_1$ and $\phi_1 = \pm \phi_2$, which, when combined with Eq.(19), results in $\Psi(3k + n) = \pm t_3/t_2 \Psi(3k - 3 + n)$. Thus midgap states exit only when $t_2 < t_3$. In general, one needs to relate ψ_{p-1} to ψ_1 . This further reduces the matrix in Eq.(20) and by defining the $(p - 2) \times (p - 2)$ matrix

$$\mathbf{h} = \begin{pmatrix} -E_m & t_1 & 0 & \dots & 0 \\ t_1 & -E_m & t_2 & \dots & 0 \\ 0 & t_2 & -E_m & \dots & \cdot \\ \dots & \dots & \dots & \dots & t_{p-3} \\ 0 & 0 & \dots & t_{p-3} & -E_m \end{pmatrix}, \quad (21)$$

we find that $\psi_1 = -t_{p-2}\mathbf{h}_{1,p-2}^{-1}\psi_{p-1}$. When combined with Eq.(19), we obtain $\psi_1 = t_{p-2}t_p/t_{p-1}\mathbf{h}_{1,p-2}^{-1}\psi_{p+1}$. Hence the midgap state with energy E_m exists only when $t_{p-2}t_p\mathbf{h}_{1,p-2}^{-1} > t_{p-1}$ ¹⁹. Note that for higher periods, commensurate structures may appear in sublattices. These structures resemble the SUSY structures in lower periods. For example, when $p = 4$, there are at most three midgap states at $E_m = 0, \pm\sqrt{t_1^2 + t_2^2}$. In this case, the Hamiltonian H_4^2 is already block diagonal in even and odd sites. For even sites, H_4^2 is period of two and belongs to H_2 with $t'_1 = t_1t_4, t'_2 = t_2t_3, \mu'_1 = t_1^2 + t_2^2$, and $\mu'_2 = t_3^2 + t_4^2$ with the midgap energy given by $E'_m = \mu'_1 = t_1^2 + t_2^2$. It is clear that E'_m is precisely the square of $E_m = \pm\sqrt{t_1^2 + t_2^2}$, and thus $\pm\sqrt{t_1^2 + t_2^2}$ are the midgap states resulting from the supersymmetry within the even sublattice. The remaining midgap state at $E_m = 0$ originates from the same supersymmetric structure as that for $p = 2$ between even and odd sites. Hence ϕ_e vanishes for $E_m = 0$. Obviously, the same effects may occur for any p that is not a prime number.

As an application, we point out that a simple way to engineer localized edge states in a nanowire (such as carbon nanotubes) is to introduce impurity-bonds periodically and form a semi-infinite superlattice structure. In this case, one has $t_1 = t_2 = \dots = t_{p-1} \equiv t$ while $t_p \equiv t'$. It is known that in the infinite case, there are p energy bands. However, when it becomes semi-infinite, $p - 1$ localized edge states may arise simultaneously and they are located exactly in the $p - 1$ gaps among these energy bands. The proposed superlattice structure thus provides a convenient way to control the number of edge states. The above result can be quite easily derived in our formulation. First of all, Eq.(20) implies that the energies of edge modes are exactly the energies of a finite atomic chain with uniform hopping t . In other words, $E = 2t \cos(ka)$ with $ka = m\pi/p, m = 1, 2, \dots, p - 1$. Note that these k 's occur exactly at the zone boundaries of the energy bands, hence they appear within the energy gaps. Eq.(19) further implies that for any edge mode, their wavefunction satisfies $\Psi(p + 1) = -t/t'\Psi(p - 1)$. Since $\Psi(1)$ and $\Psi(p - 1)$ have the same amplitude, we get $|\Psi(p + 1)| = |t/t'|\Psi(1)|$. Therefore, as long as $|t/t'| < 1$, all midgap wavefunctions decay and hence the $p - 1$ midgap states appear at the same time.

Another example is to consider the limit when p goes to infinity. Since for any given configuration of $\{t_i, i = 1, 2, 3, \dots\}$, t_i ($1 \leq i \leq p = \infty$) is allowed to be any number; effectively, the wire is a disordered semi-infinite wires. It is well known that the density of states at zero-energy become enhanced^{11,12} in the disordered wires. In the following, we will find that such enhancement can be also understood from the above point of view. Essentially, this is because for any given t_i configuration, the system has high probability to settle into the form of the ground state wavefunction discussed above. First, because the boundary breaks the translational invariance, if one decomposes the wavefunction as $\Psi = (\phi_o, \phi_e)$, it is still true that only the even sites are connected to the

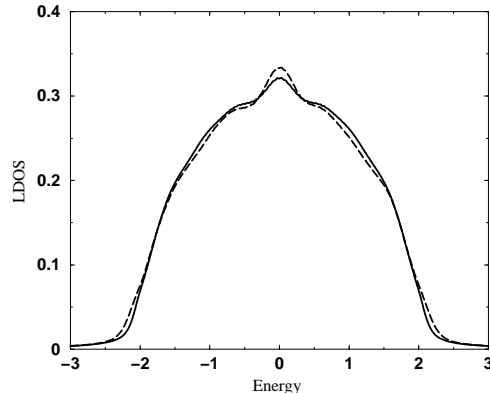


FIG. 4: Averaged local density of states over 10000 samples at the end point for semi-infinite wires with disorders near the edge point. Only 5 lattice points are imposed with disorders. Here random bonds and potentials are imposed on a uniform hopping model with $t = 1.0$, and for solid line, the amplitudes of disorders are $\delta t = 0.2$ and $\delta v = 0.2$; while for the dash line, the amplitudes of disorders are $\delta t = 0.3$ and $\delta v = 0.3$. One sees that slight disorders can induce a peak-like structure at zero energy.

hard-wall boundary point. In this case, for any set of $\{t_i\}$, the non-Hermitian matrix \mathbf{A} that enters Eq.(2) is given by

$$\mathbf{A} = \begin{pmatrix} t_1 & 0 & 0 & \dots \\ t_2 & t_3 & 0 & \dots \\ 0 & t_4 & t_5 & \dots \\ \cdot & \cdot & \cdot & \dots \end{pmatrix}. \quad (22)$$

For the zero-energy state, because $\mathbf{A}\phi_e = 0$, it is easy to see that $\phi_e = 0$; while the wavefunction at odd sites is determined by $\mathbf{A}^\dagger\phi_o = 0$. If we set $\Psi_0^1 = 1$, the wavefunction at site $2N + 1$ is given by $\Psi_0^{2N+1} \approx (t_1t_3t_5\dots t_{2N-1})/(t_2t_4t_6\dots t_{2N})$. Let $x_i \equiv |t_{2i-1}/t_{2i}|$, then $\ln|\Psi_0^{2N+1}| \approx \sum_{i=1}^N \ln x_i$. Clearly, because $\ln|\Psi_0^{2N+1}| - \ln|\Psi_0^{2N-1}| \approx \ln x_N$, the logarithm of the wavefunction at odd sites behaves effectively as a random walker. Since a random walker has large probability to go to $\pm\infty$, Ψ_0 has high probability of decaying to zero far from the edge and becomes a localized zero-energy mode. This analogy leads to $\langle(\ln|\Psi_0^{2N+1}|)^2\rangle = \sqrt{N}\sigma$ with σ being the standard deviation of $\ln x$. In other words, $|\Psi_0^{2N+1}| \sim e^{\pm\sigma\sqrt{N}}$ where \pm correspond to states localized at either ends, respectively. We emphasize that this analysis indicates that *only the standard deviation of $\ln x$ is relevant* and there is no need for the assumption of Gaussian-type randomness, which is often invoked in previous works. Furthermore, the random-walk nature makes the zero-energy peak much more easily formed. This is illustrated in Fig. 4 where we show that even slight disorders near the edge may induce features resembling zero-bias peaks in tunneling measurements. In this case, the zero-energy state tends to decay from the edge but will not become

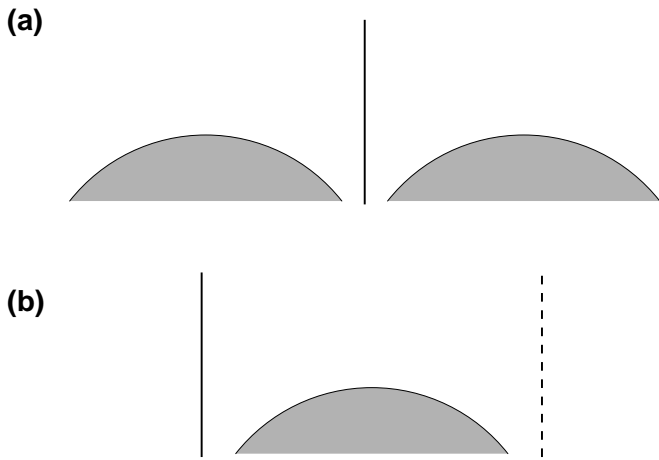


FIG. 5: Schematic plots of (a) the spectrum with a midgap state and (b) the spectrum with an impurity state, which may appear at the position of the solid line or the dashed line. Clearly, (b) may be viewed as the square of (a) (see text for details), i.e., if one folds (a) with respect to the midgap state, one gets (b).

localized. Instead, after joining the non-disorder bulk region, it becomes a resonant state²⁰. Such phenomena may have already been seen in experiments¹³.

IV. IMPURITY STATES AS MIDGAP STATES

In this section, we demonstrate that in the supersymmetric approach the ordinarily recognized impurity states can be viewed as disguised midgap states. Let us consider the Goodwin model for the surface state²¹. In this model, it was proposed that the surface state arises because the potential suddenly changes near the surface or the edge. In the tight binding limit, the Hamiltonian is given by²¹

$$H_G = \sum_{i=1}^{\infty} t c_i^\dagger c_{i+1} + h.c. + U c_1^\dagger c_1. \quad (23)$$

In other words, there is an impurity potential localized at the first site. It is commonly recognized that under appropriate condition, an impurity state (in this case, it is the Goodwin edge state.) may arise and exhibit as an isolated line in the spectrum as illustrated in Fig. 5(b). Clearly, we see from Fig. 5, the spectrum with an impurity state is essentially the square of spectrum shown in Fig. 5(a), i.e., the spectrum with a midgap state.

To establish the relation described above, we go back to previous analysis on the t_1 - t_2 model. As is obvious, the spectrum of H^S ($\equiv (H_2)^2$) is the square of that for H_2 , fulfilling the relation indicated in Fig. 5. It is hence useful and more transparent if we explicitly write down H^S

$$H^S = \begin{pmatrix} \mathbf{A}\mathbf{A}^\dagger & \mathbf{0} \\ \mathbf{0} & \mathbf{A}^\dagger\mathbf{A} \end{pmatrix}, \quad (24)$$

where

$$H_o^S = \mathbf{A}\mathbf{A}^\dagger = \begin{pmatrix} t_1^2 & t_1 t_2 & 0 & \dots \\ t_1 t_2 & t_1^2 + t_2^2 & t_1 t_2 & \dots \\ 0 & t_1 t_2 & t_1^2 + t_2^2 & \dots \\ \vdots & \vdots & \vdots & \ddots \end{pmatrix} \quad (25)$$

is the effective Hamiltonian for the odd sites and

$$H_e^S = \mathbf{A}^\dagger\mathbf{A} = \begin{pmatrix} t_1^2 + t_2^2 & t_1 t_2 & 0 & \dots \\ t_1 t_2 & t_1^2 + t_2^2 & t_1 t_2 & \dots \\ 0 & t_1 t_2 & t_1^2 + t_2^2 & \dots \\ \vdots & \vdots & \vdots & \ddots \end{pmatrix} \quad (26)$$

is the effective Hamiltonian for the even sites. One sees that H_o^S and H_e^S differ by the potential at site 1. As mentioned, this is entirely due to the missing bond cut off by the boundary. On the other hand, even though H^S is block-diagonal, it does not imply even and odd sites are independently from each other. In fact, they are connected by the supercharge H_2 . The point is that except for the zero energy which is an eigenvalue of H_o^S , H_o^S and H_e^S share the same energy eigenvalue E^2 with E being the spectrum of H_2 . The supersymmetric relation between even and odd sites enables one to solve the Goodwin model H_G as follows. One first rewrites

$$H_o^S = \sum_{i=1}^{\infty} \left[(t_1 t_2) c_i^\dagger c_{i+1} + h.c. + (t_1^2 + t_2^2) c_i^\dagger c_i \right] - t_2^2 c_1^\dagger c_1. \quad (27)$$

Clearly, it shows that the effective Hamiltonian for the odd sites is equivalent to the Goodwin model with $t = t_1 t_2$, $U = -t_2^2$, and $\mu = -(t_1^2 + t_2^2)$. The wavefunction of the midgap state on odd sites then become the wavefunction of the impurity state in the Goodwin model. Furthermore, the energy of the impurity state can be easily found to be $E_{im} = -(t_1^2 + t_2^2)$. By solving t_1 and t_2 in terms of t and U , we find $E_{im} = U + t^2/U$. Since the midgap states exist when $|t_1| < |t_2|$, the impurity state appears only when $|t| < |U|$, in consistent with the standard approach²¹. The discussion above concerns with the case $U < 0$, hence the impurity energy resides on the left side (the solid line) in Fig. 5(b). For $U > 0$, the Goodwin model maps to $-H_o^S$. One obtains the same expression for the impurity energy $E_{im} = U + t^2/U$ except that it resides on the right side (the dashed line) in Fig. 5(b).

In addition to the energy of the impurity states, the above analysis also implies that the entire spectrum is simply $E_G = 2t \cos ka$. Furthermore, the supersymmetric relation between even and odd sites enables one to write down all wavefunctions for the Goodwin model explicitly. This is entirely due to the fact that the Hamiltonian of the supersymmetric partner to the Goodwin model is H_e^S which is a uniform hopping model. We obtain the wavefunction for the impurity state $\Psi_G(n) = (t/U)^{n-1}$, while for the extended states, when $U < 0$, $\Psi_G(n) = [\sqrt{|U|} \sin nka + t/\sqrt{|U|} \sin(n-1)ka]/E_k$ with $E_k = \pm\sqrt{|U| + t^2/|U| + 2t \cos ka}$, and when $U > 0$, $\Psi_G(n) = [\sqrt{|U|} \sin nka - t/\sqrt{|U|} \sin(n-1)ka]/E_k$ with $E_k = \pm\sqrt{|U| + t^2/|U| - 2t \cos ka}$.

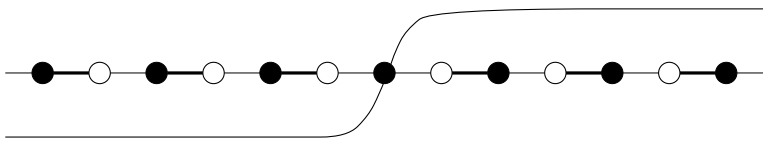
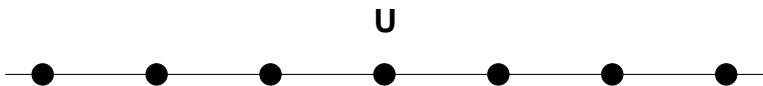
(a) Soliton**(b) Impurity**

FIG. 6: The equivalence of the electronic state in a SSH soliton background (a) and in an impurity background (b). The electronic state for an impurity resides only on the black points. In (a), the thin line represents hopping amplitude t_1 , while the thick line represents hopping amplitude t_2 . In (b), the hopping amplitude is $t_1 t_2$.

One can also apply the same approach to the bulk case. In Fig. 6(a), we show that the soliton configuration in polyacetylene discussed by Su, Schrieffer, and Heeger (the SSH soliton)^{14,17} is essentially a bulk impurity illustrated in Fig. 6(b). The same analysis leads to the results: For $U < 0$, $E_{imp} = -\sqrt{U^2 + 4t^2}$ and $\Psi_{imp}(n) = \left[|U|/(2t) - \sqrt{(U/2t)^2 + 1} \right]^{|n|}$, while for $U > 0$, $E_{imp} = \sqrt{U^2 + 4t^2}$, and $\Psi_{imp}(n) = \left[-|U|/(2t) + \sqrt{(U/2t)^2 + 1} \right]^{|n|}$. Here n is measured from the impurity site. Note that unlike the case for semi-infinite chains, the impurity state for the bulk 1D chain exists for any U and t .

The purpose of the above analysis is only for demonstration. In principle, it can be also applied to cases when the potential extends from the first to other lattice points in the Goodwin model. For instance, one can include an additional term $Vc_2^\dagger c_2$ in the Goodwin model. In that case, the first and second bonds in the corresponding t_1 - t_2 model has to be different and denoted as t'_1 and t'_2 . One then obtains that $t = t_1 t_2 = t'_1 t'_2$, $U = t'^2_1 - t_1^2 - t_2^2$, and $V = t'^2_2 - t_2^2$. Since for any changes of finite number of hoppings, the energy of the edge mode stays at zero. The energy of the impurity state is still given by $E_{imp} = -(t_1^2 + t_2^2)$. Solving t_1^2 and t_2^2 in terms of t , U , and V yields the energy of the impurity state.

We close this section by pointing out that the idea of mapping impurity states to midgap states is quite general. In addition to the simplest version of the Goodwin model discussed so far, it also works for more general cases. For instance, consider the generalized Goodwin model \tilde{H}_G in which one introduces an impurity potential at the 1st site of the t_1 - t_2 model. This model can be mapped to the effective Hamiltonian for the odd sites of a

t'_1 - t'_2 - t'_3 - t'_4 model, i.e., the $p = 4$ (H_4) model. Specifically, one finds that \tilde{H}_G is equivalent to the block in H_4 ² that describes the odd sites; while its supersymmetric partner is the original t_1 - t_2 model with no impurity potential. The impurity state of \tilde{H}_G is identified as the midgap state of the H_4 model at $E = 0$. Simple calculation then yields $E_{imp} = t_2^2/(2U) + U/2 + \sqrt{(t_2^2/(2U) + U/2)^2 + t_1^2}$. Thus, one concludes that in general the impurity state of H_p can be mapped to the midgap state of H_{2p} .

V. SUMMARY AND OUTLOOK

In summary, in this work we have shown that the properties of midgap states in semi-infinite 1D nanowires are dictated by an underlying discrete supersymmetry. This supersymmetric structure generalizes the ordinary supersymmetric quantum mechanics and offers a new point of view toward the origin of edge states. In the presence of hard-wall boundary condition ($\psi = 0$), the sublattice which directly connects to the hard-wall spans the null space of the supersymmetric ground state. As a consequence, the energies of the midgap states are determined by the eigenvalues of a reduced Hamiltonian, Eq.(20), whose size is much smaller than that of the original Hamiltonian. This reduction in matrix size significantly reduces the computation cost for determining the occurrence of the midgap states and offers a way to manipulate them. As an application, we investigate a structure with superlattice in hopping. In this case, the number of edge states is simply the period of the superlattice minus one. Therefore, changing the period offers a way to control the number of localized electronic states at the edge of the nanowires.

While so far in this work we have not considered electron-electron interactions, from adiabatic continuity, the results obtained here should still hold for cases when the electron-electron interactions are weak (so that quasi-particles are well defined). Moreover, if the “1D chain” results from the reduction of a higher dimensional structure where interactions are not important, then it is legitimate to ignore interactions in its effective 1D model. This is of course not correct in truly 1D atomic chains where it is known that interactions may dominate the physics and the quasi-particle pictures may fail. In this case, however, the states we obtain can be used as the basis to express the full Hamiltonian (with interactions) utilizing the relation $c_{i\sigma}^\dagger = \psi_0(i)c_{0\sigma}^\dagger + \sum_E \psi_E(i)c_{E\sigma}^\dagger$. When Coulomb interaction is included, it reduces to the Anderson model²² in which the edge state acts as an impurity state. The scattering of extended states by the edge states essentially causes the Kondo effect, resulting in the zero-bias peaks near the Fermi energies⁴. On the other hand, the interaction also correct the localized edge state. This is conventionally analyzed in the Fano-Anderson model²², in which it is known that as long as the new energy found remains inside the gap, the corresponding state is a localized state. In either of the above

mentioned effects, our results will serve as useful inputs for attaining the final corrections.

Acknowledgments

We gratefully acknowledge discussions with Profs. Sungkit Yip, Hsiu-Hau Lin, and T. K. Lee and support from the National Science Council of the Republic of China under Grant Nos. NSC 92-2112-M-007-038.

APPENDIX A: SUPERALGEBRA IN INFINITE p -PARTITE SYSTEMS

In this appendix, detailed superalgebra behind our generalized SUSY quantum mechanics is presented. For an infinite p -partite system, after modulo p , the system reduces to the set $\{1, 2, 3, \dots, p\}$ with each number representing different sublattices. The reduced system is periodic with $p+1$ being identified as 1. In this periodic space, a set of generators $\{Q_{nm}; n, m = 1, 2, \dots, p\}$ can be defined. Here Q_{nm} are $p \times p$ Hermitian matrices whose only nonvanishing elements are 1 in the n th row and m th column and the m th row and n th column. Note that Q_{nn} has only one element, 1, in the n th element along the diagonal. Obviously, when $n \neq m$, Q_{nm} permutes the subwavefunctions ϕ_n and ϕ_m ; when combined with the hopping strength t_{nm} , in addition to permutation, it also rescales the wavefunctions. The Lie algebra formed by Q_{nm} is a superalgebra because the anticommutator is necessary in order to be closed. The followings are nontrivial commutation relations: $\{Q_{lm}, Q_{mn}\} = Q_{ln}$ for $l \neq n$, $\{Q_{nm}, Q_{nm}\} = 2Q_{nn} + 2Q_{mm}$ for $n \neq m$, and $[Q_{nm}, Q_{mm}] = \delta_{nm}Q_n$; all the other commutators are zero. It is straightforward to check that for infinite systems, the SUSY Hamiltonian H_S defined in Sec.III commutes with all Q_{nm} even if the operation of modulo p is not performed.

APPENDIX B: DERIVATION OF $[H_S, Q_p] = 0$

In this appendix, we outline the proof of $[H_S, Q_p] = 0$ for semi-infinite chains. We first write $Q_p = q_p + q_p^\dagger$ where q_p is obtained by setting the last column in Q_p to zero in

Eq.(18). It is then suffice to prove $[H_S, q_p] = 0$. We note that H_S has the following generic form

$$H_S = \begin{pmatrix} \mathbf{S}_{11} & \mathbf{S}_{12} & \mathbf{S}_{13} & \cdots & \mathbf{0} \\ \mathbf{S}_{21} & \mathbf{S}_{22} & \mathbf{S}_{23} & \cdots & \mathbf{0} \\ \mathbf{S}_{31} & \mathbf{S}_{32} & \mathbf{S}_{33} & \cdots & \cdot \\ \cdots & \cdots & \cdots & \mathbf{S}_{p-1,p-1} & \mathbf{0} \\ \mathbf{0} & \mathbf{0} & \cdots & \mathbf{0} & \mathbf{0} \end{pmatrix} + H_S^0 \equiv \left(\begin{array}{c|c} \mathbf{H}^+ & \mathbf{0} \\ \hline \mathbf{0} & \mathbf{H}^- \end{array} \right) \quad (\text{B } 1)$$

Here H_S^0 has the same form as that of the SUSY Hamiltonian for the corresponding infinite chain except that semi-infinite lattice points are removed, hence it is block-diagonal with the form: $(H_S^0)_{nm} = \mathbf{S}_0 \delta_{nm}$, where n and m are the block indices and

$$\mathbf{S}_0 = \begin{pmatrix} 0 & t & 0 & \cdots & 0 \\ t & 0 & t & \cdots & 0 \\ 0 & t & 0 & \cdots & \cdot \\ \cdots & \cdots & \cdots & \cdots & t \\ 0 & 0 & \cdots & t & 0 \end{pmatrix} \quad (\text{B } 2)$$

and $t = t_1 t_2 t_3 \cdots t_p$. The block matrix \mathbf{S}_{nm} represents *missing* hopping amplitudes that goes between sublattices m and n due to the presence of the boundary point at $i = 0$. When computing $[H_S, q_p]$, one needs to compute $[\mathbf{S}_0, \mathbf{A}_{1p}^\dagger]$, $\mathbf{A}_{1p}^\dagger \cdot \mathbf{S}_{1m}$ and $\mathbf{A}_{p-1,p}^\dagger \cdot \mathbf{S}_{p-1,m}$, thus only \mathbf{S}_{1m} and $\mathbf{S}_{p-1,m}$ are needed. It is straightforward to show that $[\mathbf{S}_0, \mathbf{A}_{1p}^\dagger]$ has only one element $-tt_p$, which is the 1st element along the diagonal ($\equiv \delta_{11}$). To obtain \mathbf{S}_{nm} , one needs to multiply H_p to itself by n ($\leq p$) times because H_S is a polynomial of H_p containing at most p th power of H_p . Now the multiplication of H_p to itself n times effectively hops a particle n times. Since $n \leq p$, only when the particle starts from the lattice points $1 \leq i \leq p-1$, it will have chance to visit $i = 0$ and thus will have missing paths when $i = 0$ is removed. It implies that all \mathbf{S}_{nm} have only one element, which is also the 1st element along the diagonal. In addition, $\mathbf{S}_{p-1,m} = 0$ for $m \geq 2$. As a result, by using Eq.(16), we obtain $\mathbf{A}_{1p}^\dagger \cdot \mathbf{S}_{1m} = 0$ and hence we only need to compute $\mathbf{S}_{p-1,1}$. Since the only missing path between the point 1 and the point $p-1$ is $1 \rightarrow 0 \rightarrow 1 \rightarrow 2 \cdots \rightarrow p-1$, we find that $\mathbf{S}_{p-1,1}$ is $-t_p^2 t_1 t_2 \cdots t_{p-1} \delta_{11}$. This result, when combined with $[\mathbf{S}_0, \mathbf{A}_{1p}^\dagger] = -tt_p \delta_{11}$, we finally obtain $[H_S, Q_p] = 0$.

¹ See for instance, Joachim and Roth, *Atomic and Molecular Wires* (Kluwer Academic Publishers, Boston, 1997), and more recently, N. Nilius, T. M. Wallis, and W. Ho, *Science* **297**, 1853 (2002).

² B. I. Halperin, *Phys. Rev. B* **25**, 2185 (1982) and X. G. Wen, *Phys. Rev. B* **43**, 11025 (1991).

³ S. T. Wu and C.-Y. Mou, *Phys. Rev. B* **66**, 012512 (2002); **67**, 024503 (2003); *Physica C* **388-389**, 45 (2003).

⁴ For externally-introduced cases, see, for example, Y. Meir,

N. S. Wingreen, and P. A. Lee, *Phys. Rev. Lett.* **70**, 2601(1993); Cronenwett *et al.*, *Science* **281**, 540 (1998).

⁵ Y. Shibayama, H. Sato, T. Enoki, and M. Endo, *Phys. Rev. Lett.* **84**, 1744 (2000).

⁶ T. Hikihara, X. Hu, H. H. Lin and C.-Y. Mou, *Phys. Rev. B* **68**, 035432 (2003).

⁷ See for example, K. Efetov, *Supersymmetry in Disorder and Chaos* (Cambridge Univ Press, 1999).

⁸ See for example, G. Junker, *Supersymmetric Methods in*

Quantum and Statistical Physics (Springer, New York, 1996).

- ⁹ I. Kosztin, S. Kos, M. Stone, and A. J. Leggett, *Phys. Rev. B* **58**, 9365 (1998); I. Adagideli, P. M. Goldbart, A. Shnirman, and A. Yazdani, *Phys. Rev. Lett.* **83**, 5571 (1999).
- ¹⁰ See, for instance, S. Durand, *Phys. Lett. B* **312**, 115(1993). Another generalization that is often discussed is the para-supersymmetry. See, for example, K. Samani and A. Mostafazadeh, *Nucl. Phys. B* **595**, 467 (2001), and reference therein.
- ¹¹ See, for example, R. H. McKenzie, *Phys. Rev. Lett.* **77**, 4804 (1996); L. Balents and M. P. A. Fisher, *Phys. Rev. B* **56**, 12970 (1997), and references therein.
- ¹² F. J. Dyson, *Phys. Rev.* **92**, 1331 (1953).
- ¹³ See, for example, H. W. Cheng and C. C. Chi, *J. Low Temp. Phys.* **131**, 477 (2003).
- ¹⁴ W. P. Su, J. R. Schrieffer, and A. J. Heeger, *Phys. Rev. Lett.* **42**, 1698 (1979).
- ¹⁵ H.H. Lin, unpublished, (2004).
- ¹⁶ The construction of H_S essentially used the Hamilton-Cayley theorem often quoted in elementary linear algebra. Here for the purpose of reference, we list some of its forms: $p = 3$: $H_S = H_p^3 - (t_1^2 + t_2^2 + t_3^2)H_p$; $p = 4$:
 $H_S = H_p^4 - (t_1^2 + t_2^2 + t_3^2 + t_4^2)H_p^2 + t_2^2 t_4^2 + t_1^2 t_3^2$. Clearly, for higher p , it involves higher powers of H_p .
- ¹⁷ W. P. Su and J. R. Schrieffer, *Phys. Rev. Lett.* **46**, 738 (1981).
- ¹⁸ Because ϕ_p is an eigenstate to \mathbf{H}^- with eigenvalue E_S and \mathbf{H}^- is a uniform hopping model, ϕ_p is either in the form of $\sin(npka)$ or simply zero. Since $\phi_p = \sin(npka)$ is an extended state, the only possibility for accommodating the midgap states is $\phi_p = 0$. Therefore, $\phi_p = 0$ and the following construction exhaust all possibilities.
- ¹⁹ This is equivalent to find the number of midgap states. Using \mathbf{H}^+ and \mathbf{H}^- , the number of midgap states can be formally counted. For instance, if one defines the index as $\text{ind}(z) \equiv \text{Tr} \left(\frac{z}{z+\mathbf{H}^+} - \frac{z}{z+\mathbf{H}^-} \right) + \text{Tr} \left(\frac{\mathbf{H}^+}{z+\mathbf{H}^+} - \frac{\mathbf{H}^-}{z+\mathbf{H}^-} \right)$, $\text{ind}(0)$ gives the number of midgap states.
- ²⁰ For non-disordered carbon nanotubes, resonant states have been observed in P. Kim, T. W. Odom, J.-L. Huang, and C. M. Lieber, *Phys. Rev. Lett.* **82**, 1225 (1999).
- ²¹ T. Heinzl, *Mesoscopic Electronics in Solid State Nanostructures* (Wiley-VCH, 2003), Chapter 3.
- ²² G. D. Mahan, *Many-Particle Physics* (2nd Edition, Plenum Press, New York, 1990), Sections 1.4B and 4.2.